Acta Biomaterialia 9 (2013) 5728–5739

Incorporation of bioactive glass in calcium phosphate cement: An evaluation

A.C.M. Renno [a,b], F.C.J. van de Watering [a], M.R. Nejadnik [a], M.C. Crovace [c], E.D. Zanotto [c], J.G.C. Wolke [a], J.A. Jansen [a], J.J.J.P. van den Beucken [a,*]

[a] Department of Biomaterials (309), Radboud University Nijmegen Medical Center, P.O. Box 9101, 6500 HB Nijmegen, The Netherlands
[b] Department of Bioscience, Federal University of São Paulo (UNIFESP), Av. Ana Costa, 95, Santos, SP 11050240, Brazil
[c] Department of Material Engineering, Federal University of São Carlos (UFSCar), Rodovia Washington Luís (SP-310), Km 235, 16015-223, São Carlos, SP, Brazil

ARTICLE INFO

Article history:
Received 14 June 2012
Received in revised form 1 November 2012
Accepted 5 November 2012
Available online 14 November 2012

Keywords:
Bone substitute
Calcium phosphate cement
Bioactive glass
In vivo

ABSTRACT

Bioactive glasses (BGs) are known for their unique ability to bond to living bone. Consequently, the incorporation of BGs into calcium phosphate cement (CPC) was hypothesized to be a feasible approach to improve the biological performance of CPC. Previously, it has been demonstrated that BGs can successfully be introduced into CPC, with or without poly(D,L-lactic-co-glycolic) acid (PLGA) microparticles. Although an in vitro physicochemical study on the introduction of BG into CPC was encouraging, the biocompatibility and in vivo bone response to these formulations are still unknown. Therefore, the present study aimed to evaluate the in vivo performance of BG supplemented CPC, either pure or supplemented with PLGA microparticles, via both ectopic and orthotopic implantation models in rats. Pre-set scaffolds in four different formulations (1: CPC; 2: CPC/BG; 3: CPC/PLGA; and 4: CPC/PLGA/BG) were implanted subcutaneously and into femoral condyle defects of rats for 2 and 6 weeks. Upon ectopic implantation, incorporation of BG into CPC improved the soft tissue response by improving capsule and interface quality. Additionally, the incorporation of BG into CPC and CPC/PLGA showed 1.8- and 4.7-fold higher degradation and 2.2- and 1.3-fold higher bone formation in a femoral condyle defect in rats compared to pure CPC and CPC/PLGA, respectively. Consequently, these results highlight the potential of BG to be used as an additive to CPC to improve the biological performance for bone regeneration applications. Nevertheless, further confirmation is necessary regarding long-term in vivo studies, which also have to be performed under compromised wound-healing conditions.

1. Introduction

Apatite cements (such as calcium phosphate cement, CPC) represent a promising candidate material for bone substitution, mainly due to their biocompatibility and osteoconductive properties [1–5]. An additional advantage of such cements is their self-setting nature, which makes them injectable and allows the use of a minimally invasive surgical procedure during clinical use [2,4,5]. However, CPCs are characterized by a very slow degradation rate, which has to be considered as a disadvantage for several applications, like sinus elevation and the filling of extraction sockets [1,5].

To enhance the biodegradability and tissue ingrowth of CPC, (micro)porosity can be introduced into the already intrinsically nanoporous cement [1,5]. One promising strategy to create porosity into CPC is the introduction of biodegradable polymers, e.g. in the form of poly(D,L-lactic-co-glycolic) acid (PLGA) microparticles [6–9]. PLGA microparticles degrade over time and hence create pores within the ceramic matrix that increase the surface-to-volume ratio of the CPC and allow tissue ingrowth [10,11]. Many animal studies demonstrated that porosity created by degradation of PLGA microparticles embedded within CPC increases cement degradation and accelerates the regeneration of a bone defect [9–12]. However, the osteoconductive properties of CPC/PLGA are not sufficient to achieve complete defect filling under critical conditions, like poorly vascularized sites and (elderly) patients with metabolic disorders [13]. Consequently, the enrichment of CPC/PLGA with osteopromotive or osteoinductive factors is necessary to improve their biological performance.

Bioactive glasses (BGs) are a group of synthetic silica-based bioactive materials with the unique ability to bond to living bone by forming a biologically active bone-like apatite layer on their surface [14–17] that acts as a template for calcium phosphate precipitation and directs new bone formation [14,17,18]. In addition, it has been suggested that BGs stimulate osteoprogenitor cells to differentiate into matrix-producing osteoblasts and subsequently increase the rate of bone formation and bone ingrowth into BG-based granular material [19–21]. In view of this, the incorporation of BG into CPC seems a safe approach to improve the osteopromotive properties of CPC.

* Corresponding author. Tel.: +31 24 3667305; fax: +31 24 3614657.
E-mail address: j.vandenbeucken@dent.umcn.nl (J.J.J.P. van den Beucken).

1742-7061/$ - see front matter © 2012 Acta Materialia Inc. Published by Elsevier Ltd. All rights reserved.
http://dx.doi.org/10.1016/j.actbio.2012.11.009

In a recent in vitro study, we demonstrated that BG can successfully be introduced into CPC and CPC/PLGA composites, with a maximum of 30 wt.% BG, without compromising the setting time and mechanical properties of CPC or CPC/PLGA composites. Furthermore, BG has been shown to desirably counteract the acidity provoked by brushite cements in an in vitro study [22]. Together, these encouraging in vitro data on the introduction of BG into CPC composite material formed the basis for the current in vivo study, which aimed to evaluate the ectopic and orthotopic in vivo response to CPC/BG composites, with or without PLGA microparticles, in rats. Pre-set scaffolds in four different formulations (1: CPC; 2: CPC/BG; 3: CPC/PLGA; and 4: CPC/PLGA/BG) were implanted subcutaneously and in femoral condyle defects of rats. Histocompatibility (ectopic implants; histology) and bone responses (orthotopic implants; histology and histomorphometry) were evaluated after 2 and 6 weeks of implantation.

2. Materials and methods

2.1. Materials

Calcium phosphate cement consisted of 85% alpha-tricalcium phosphate (α-TCP; CAM Bioceramics BV, Leiden, The Netherlands), 10% dicalcium phosphate anhydrous (DCPA; J.T. Baker Chemical Co., USA) and 5% hydroxyapatite (HA; Merck, Darmstadt, Germany). For the preparation of the cement, 2% Na_2HPO_4 was used as the liquid phase. Acid-terminated poly(D,L-lactic-co-glycolic acid) (PLGA; Purasorb®, Purac, Gorinchem, The Netherlands) with a lactic-to-glycolic-acid ratio of 50:50 and a molecular weight (M_w) of 17 kDa was used for microparticle preparation. Biosilicate® parent glass (fully crystallized bioactive glass ceramic of the quaternary Na_2O–CaO–SiO_2–P_2O_5 system) was provided by Vitreous Materials Laboratory (LaMaV), Department of Materials Engineering, Federal University of São Carlos, São Carlos, São Paulo, Brazil [23].

2.2. Preparation of dense PLGA microparticles

Dense PLGA microparticles were prepared by a single emulsion technique, as described previously [3]. Briefly, 0.2 g of PLGA was dissolved in 2 ml of dichloromethane (DCM) (Merck, Darmstadt, Germany) in a 20 ml glass tube. A 2 ml aliquot of this solution was transferred to a stirred beaker containing 100 ml of 0.3% poly (vinyl alcohol) (PVA) (88% hydrolyzed, MW 22000, Acros, Geel, Belgium) solution. Subsequently, 50 ml of 2% isopropanol (IPN) (Merck) was added. The solution was stirred for 1 h. The microparticles were allowed to settle for 1 h and the clear solution was decanted. The suspension left was centrifuged and the clear solution on top was aspirated. Finally, the microparticles were washed and collected through centrifugation at 1500 rpm for 5 min, lyophilized and stored at −20 °C until use. The size distribution of the microparticles was determined by image analysis (Leica Qwin®, Leica Microsystems, Wetzlar, Germany). The microparticles were imaged by scanning electron microscopy (SEM; JEOL6310 at 15 kV).

2.3. Preparation of the pre-set composites

Four experimental groups were created: (1) CPC, (2) CPC/BG, (3) CPC/PLGA and (4) CPC/PLGA/BG. Table 1 represents an overview of the composition of these materials.

For both subcutaneous and femoral implants, pre-set composites were made by adding different amounts of the base materials inside a 2 ml closed tip syringe (BD Plastipakt, Becton Dickinson SA, Madrid, Spain; Table 1) and pre-mixing the powder mixture using a mixing apparatus (Silamat, Vivadent, Schaan, Liechtenstein). Subsequently, a Na_2HPO_4 solution (2 wt.%) in a liquid/powder ratio of 0.35 was added into the syringe and the mixtures were mixed for another 20 s. Directly after mixing, the composite cements were injected into Teflon molds (3 mm × 2.9 mm). After overnight setting at room temperature, the pre-set composites were removed from the molds and analyzed using SEM. Before use, the pre-set composites were sterilized by γ-radiation with a minimum dose of 25 kGy (Isotron BV, Ede, The Netherlands).

2.4. Characterization of pre-set composites

2.4.1. Chemical analysis

Attenuated total reflection Fourier transform infrared spectroscopy (ATR-FTIR, Perkin Elmer, Spectrum One, Groningen, The Netherlands) spectra of CPC, BG, PLGA and the composites were obtained. In addition, X-ray diffraction (XRD, Philips, Cu-Ka, 45 kV, 30 mA) patterns of the CPC, BG and CPC/BG composite were collected in the 2θ range of 20–60° and were used to evaluate the potential crystalline phases available in the composite.

2.4.2. Porosity measurements

The microporosity (i.e. additional porosity after PLGA microparticles degradation) and total porosity (i.e. intrinsic porosity/microporosity) were determined by measuring the weight of pre-set composite cylinders, with and without PLGA microparticles. To burn out the PLGA microparticles, composite scaffolds were placed in a furnace at 650 °C for 2 h. Subsequently, microporosity and total porosity were calculated using the following equations [1]:

$$\varepsilon_{tot} = \left(1 - \frac{m_{burnt}}{V * \rho_{HAP}}\right) * 100\% \quad (1)$$

$$\varepsilon_{micro} = \left(1 - \frac{m_{burnt}}{m_{nanoporous}}\right) * 100\% \quad (2)$$

where ε_{tot} is total porosity (%), ε_{micro} is microporosity (%) m_{burnt} is average mass sample (after burning out polymer) (g), $m_{nanoporous}$ is average mass intrinsic nanoporous sample (g), V is volume sample (cm^3) and ρ_{HAP} is density hydroxyl apatite (g cm^{-3}).

2.5. Surgical procedure

Twenty-four healthy young adult male Wistar rats (12 weeks old; weight 295 ± 29 g) were used as experimental animals. The animal experimental plan was reviewed and approved by the Experimental Animal Committee of the Radboud University (RU-DEC 2011-156) and national guidelines for the care and use of laboratory animals were observed.

Anesthesia was induced and maintained by Isoflurane inhalation (Rhodia Organique Fine Ltd.). To minimize post-operative discomfort, buprenorfine (Temgesic; Reckitt Benckiser Health Care Ltd., Schering-Plough, Hoddesdon, UK) was administered intraperitoneally (0.02 mg kg^{-1}) directly after the operation and subcutaneously for 2 days after surgery.

To insert implants into the femoral condyles, the animals were immobilized on their back and both hind limbs were shaved, washed and disinfected with povidone–iodine. After exposure of the distal femoral condyle, a 1.0 mm pilot hole was drilled. The hole was gradually widened with drills of increasing size until a final defect size of 3 mm in width and 3 mm in depth was reached. Low rotational drill speeds (max. 450 rpm) and constant physiologic saline irrigation were used. After preparation, the defects were thoroughly irrigated and packed with sterile cotton gauze to stop bleeding. Surgery was performed in both legs of the rats and one defect was created in each condyle. The pre-set implants were placed in the created defect, according to a randomization scheme (n = 6 per experimental group, per time point). Thereafter,

Table 1
Composition and porosity values of pre-set composite materials.

Groups	CaP (wt.%)	BG (wt.%)	PLGA (wt.%)	Macroporosity	Total porosity
CPC	100	0	0	–	40.6 ± 0.7
CPC/BG	70	30	0	–	41.6 ± 0.8
CPC/PLGA	70	0	30	40.5 ± 1.2	55.7 ± 0.9
CPC/PLGA/BG	40	30	30	41.2 ± 0.8	56.5 ± 1.5

CPC, calcium phosphate cement; BG, bioactive glass; CPC/BG, BG incorporated into CPC; CPC/PLGA, dense PLGA microparticles incorporated into CPC; CPC/PLGA/BG, dense PLGA microparticles and BG incorporated into CPC.

Table 2
Modified histological grading scale for soft tissues.

Evaluation	Response	Score
Capsule thickness	1–4 cell layers	4
	5–9 cell layers	3
	10–30 cell layers	2
	>30 cell layers	1
	Not applicable	0
Tissue response of the capsule surrounding the implants	Fibrous, mature, not dense, resembling connective or fat tissue in the noninjured regions	4
	Fibrous, but immature, showing fibroblasts and little collagen	3
	Granulous and dense, containing both fibroblasts and many inflammatory cells	2
	Consists of masses of inflammatory cells with little or no signs of connective tissue organization	1
	Cannot be evaluated because of infection or factors not necessarily related to the material	0
Tissue response directly adjacent to the implant surface (interface)	Fibroblasts contact the implant surface without the presence of macrophages or foreign body giant cells	4
	Scattered foci of macrophages and foreign body cells are present	3
	One layer of macrophages and foreign body cells is present	2
	Multiple layers of macrophages and foreign body cells are present	1
	Cannot be evaluated because of infection or other factors not necessarily related to the material	0

the wound was closed with resorbable Vicryl® 5-0 (Johnson & Johnson, St. Stevens-Woluwe, Belgium), after which the skin was closed by staples (Agraven®; InstruVet BV, Cuijk, The Netherlands).

In addition, half of the animals (12 rats) received four pre-set implants placed subcutaneously into the back of each rat. To insert the implants, rats were immobilized on their abdomen and the skin was shaved, washed and disinfected with iodine. Four paravertebral incisions were made (two on each site of the vertebral column) and subcutaneous pockets were created by blunt dissection. The implants were randomly placed for each group ($n = 6$ per experimental group, per time point). Finally, the skin was closed using staples (Agraven®, Instruvet BV). The animals were housed in pairs and the intake of water and food was monitored in the initial postoperative period. Further, the animals were observed for signs of pain, infection and proper activity. After 2 and 6 weeks of implantation, rats were sacrificed by CO_2 suffocation.

2.6. Histological procedures

After harvesting the specimens (the subcutaneous implants and femoral condyles), the specimens were fixated in 4% formaldehyde for 2 days, followed by dehydration in a graded series of ethanol and embedding in methylmethacrylate (MMA). After polymerization of the specimens, histological analysis was done. Therefore, for both subcutaneous implants and femoral condyles, thin sections (10 μm) were prepared perpendicular to the medial–lateral drilling axis of the implants using a microtome with a diamond blade (Leica Microsystems SP 1600, Nussloch, Germany) [24]. At least three sections of each specimen were stained with methylene blue and basic fuchsin.

2.7. Histological and histomorphometrical evaluation

A histological grading scale was used to evaluate the capsule thickness, tissue response of the capsule surrounding the subcutaneous implants and the tissue directly adjacent to the implant surface in four pre-determined fields (superior, inferior, right and left regions of the implant) using light microscopy as previously reported (Table 2) [25,26]. At least three sections of each specimen were examined using light microscopy (Leica Microsystems AG, Wetzlar, Germany). Two experienced observers (AR and FW) performed the scoring in a blinded manner.

The femoral condyle defects were quantitatively scored using computer-based image analysis techniques (Leica® Qwin Pro-image analysis system, Wetzlar, Germany) by defining a 3 mm diameter circular area (i.e. the diameter of the created defects) superimposed on the bone defect area as the region of interest (ROI). From digital images (magnification 2.5×), the amount of CPC and bone tissue within this ROI were determined [9].

2.8. Statistical analysis

Statistical analyses of material degradation and bone formation were performed using SPSS, version 16.0 (SPSS Inc., Chicago, IL, USA). The statistical comparisons were performed using a one-way analysis of variance (ANOVA) with a Tukey multiple comparison post-test. Differences were considered significant at P-values <0.05.

3. Results

3.1. Materials characterization

Morphological examination of BG granulate revealed that the BG particles had an irregular structure with an average particle size of ~2.5 ± 0.2 μm (Fig. 1A). The preparation of PLGA microparticles via the single-emulsion solvent-extraction technique resulted in PLGA microparticles with an average size of 40 ± 4 μm. Morphological examination using SEM revealed that the PLGA microparticles had a spherical appearance with a smooth surface (Fig. 1B). Fig. 1C

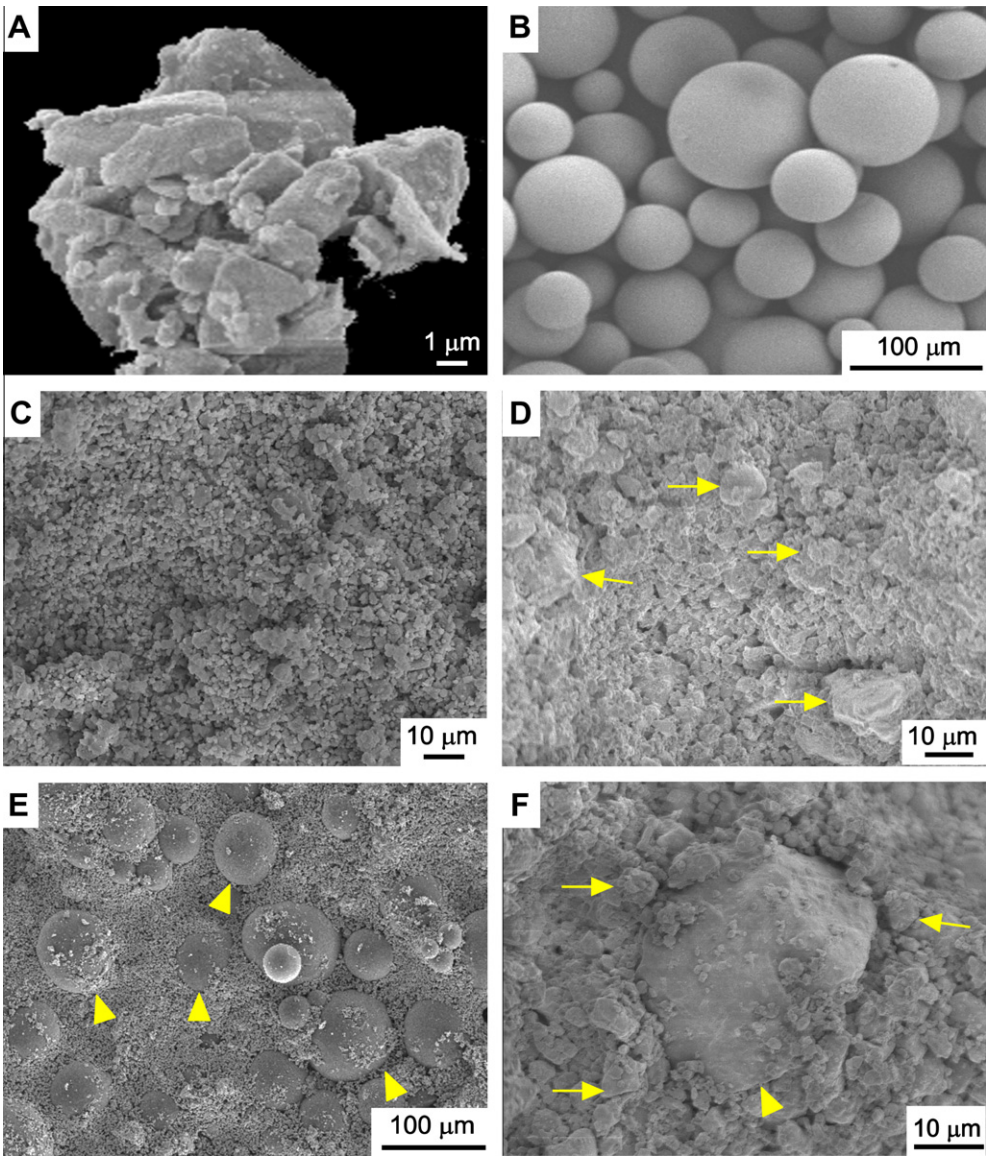

Fig. 1. SEM micrographs of the (A) BG particles, (B) dense PLGA microparticles, (C) CPC, (D) CPC/BG, (E) CPC/PLGA and (F) CPC/PLGA/BG. BG (arrow) and PLGA microparticles (arrowheads) are indicated in the SEM micrographs. Bar represents 1, 10 or 100 μm.

represents the SEM evaluation of the CPC surface structure. Surface examination of CPC/BG, CPC/PLGA and CPC/PLGA/BG with SEM showed homogenous distribution of BG granulate and/or PLGA microparticles within CPC, respectively (Fig. 1D–F). ATR-FTIR spectra of the materials (Fig. 2A) allowed for detection of CPC, BG and PLGA in the corresponding composites. Specifically the strong peak of carbonyl at 1750 cm^{-1} was apparent in PLGA containing samples while a combination of peaks at the range of 900 to 1100 cm^{-1} represented the PO_4^{3-} and SiO_2 groups of CPC and BG in the corresponding composites. Similarly, XRD patterns of CPC/BG composite (Fig. 2B) contained the characteristic peaks of both CPC and BG.

Porosity measurements demonstrated total porosity values (due to intrinsic nanoporosity) of 40.6 ± 0.7% and 41.6 ± 0.8% for CPC and CPC/BG, respectively. Composite cements containing PLGA microparticles showed values of 40.5 ± 1.2% (microporosity) and 55.7 ± 0.9% (total porosity) for CPC/PLGA and 41.2 ± 0.8% (microporosity) and 56.5 ± 1.5% (total porosity) for CPC/PLGA/BG (Table 1).

3.2. General observation of the experimental animals

From the 24 animals used in this study, two animals were lost due to an anesthesia-induced respiratory depression, of which one animal received two femoral condyle implants and the second animal received two femoral condyle implants and four subcutaneous implants. The remaining animals recovered uneventfully from the surgical procedure and remained in good health during the entire implantation period. No clinical sign of inflammation or adverse tissue response was observed during the implantation period. At the end of the experiment, 44 subcutaneous implants were retrieved, of which 43 were used for analysis (1 CPC/PLGA/BG implant was excluded from analysis due to implant fracturing during histological processing). Furthermore, a total of 44 femoral condyle implants were retrieved and all of them were included for analyses. An overview of the number of implants placed, retrieved and used for analysis is presented in Table 3.

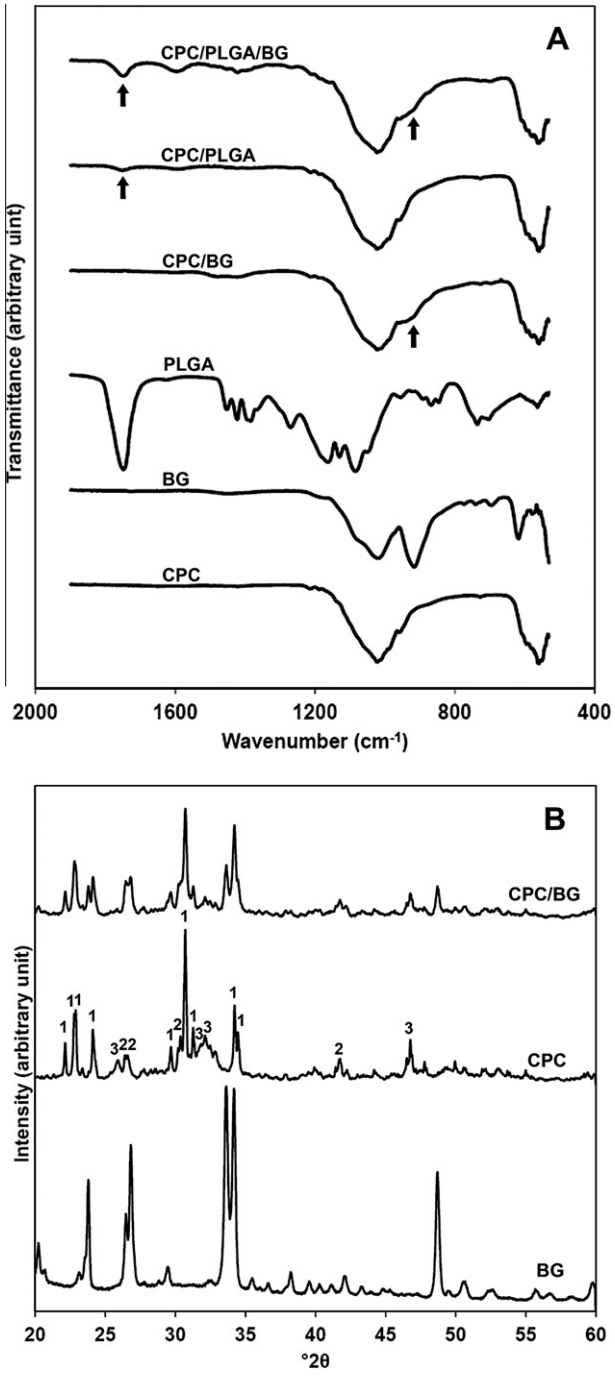

Fig. 2. ATR-FTIR spectra of CPC, BG, PLGA, CPC/BG, CPC/PLGA and CPC/BG/PLGA (A). Arrows point the peaks associated with BG and/or PLGA in the composites. X-ray diffraction patterns of BG and CPC as well as the CPC/BG composite (B). Characteristic peaks of α-TCP, DCPA and HA are marked with numbers 1, 2 and 3, respectively.

3.3. Descriptive histology of subcutaneous implants

3.3.1. Two weeks

Representative histological sections of all experimental groups 2 weeks after implantation are depicted in Fig. 3.

CPC and CPC/BG revealed no sign of material degradation and the implants were visual as a dense material (Fig. 3A and C). CPC/PLGA showed PLGA microparticle degradation, which was visualized by the formation of pores within the material (Fig. 3E). CPC/PLGA/BG revealed clear degradation and changes in the morphological shape of the implants (Fig. 3G).

At a higher magnification, CPC, CPC/BG, CPC/PLGA/BG implants were found to be surrounded by a medium-thick granulous capsule of 10–30 cell layers containing moderate numbers of inflammatory cells and fibroblasts (Fig. 3B, D and H). CPC/PLGA showed the presence of a granulous capsule consisting of more than 30 cell layers, and large numbers of inflammatory cells were present within the capsule (Fig. 3F). Directly adjacent to the surface of the CPC, CPC/BG and CPC/PLGA/BG implants (interface), moderate numbers of multi-nucleated giant cells were observed, while at the interface of CPC/PLGA, many multi-nucleated giant cells were seen.

Table 3
Number of implants placed, retrieved and used for histological analyses for the subcutaneous implants and femoral condyle defect implants.

	Implants placed		Implants retrieved		Implants used for analysis	
	Week 2	Week 6	Week 2	Week 6	Week 2	Week 6
Subcutaneous implants						
CPC	6	6	5[a]	6	5	6
CPC/BG	6	6	5[a]	6	5	6
CPC/PLGA	6	6	5[a]	6	5	6
CPC/PLGA/BG	6	6	5[a]	6	5	5[b]
Femoral condyle implants						
CPC	6	6	5[a]	6	5	6
CPC/BG	6	6	5[a]	6	5	6
CPC/PLGA	6	6	6	5[a]	6	5
CPC/PLGA/BG	6	6	6	5[a]	6	5

CPC, calcium phosphate cement; BG, bioactive glass; CPC/BG, BG incorporated into CPC; CPC/PLGA, dense PLGA microparticles incorporated into CPC; CPC/PLGA/BG, dense PLGA microparticles and BG incorporated into CPC.

[a] Deviation from number of implants placed due to animal dead.

[b] Deviation from number of implants retrieved due to fracturing of implants during to the histological processing.

3.3.2. Six weeks

Representative histological sections of all experimental groups 6 weeks after implantation are depicted in Fig. 4.

CPC and CPC/BG revealed no sign of material degradation and the implants were visual as dense material (Fig. 4A and C). Implant degradation had continued for CPC/PLGA and CPC/PLGA/BG, showing most degradation in the periphery of CPC/PLGA (Fig. 4E) with the larger extent of degradation for CPC/PLGA/BG (Fig. 4G). Additionally, CPC/PLGA and CPC/PLGA/BG showed tissue ingrowth in the degrading areas of the implant.

At higher magnification, all experimental groups revealed a thinner capsule surrounding the implant compared to their 2-weeks-implanted equivalents with a capsule thickness of 5–9 cell layers for CPC and 1–4 cell layers for the other formulations. The capsules surrounding CPC and CPC/BG consisted of fibroblasts (Fig. 4B and D). CPC/PLGA and CPC/PLGA/BG implants were surrounded by a mature fibrous capsule which resembled connective tissue in the non-injured regions (Fig. 4F and H). For CPC, CPC/BG and CPC/PLGA implants, still multi-nucleated giant cells were present at the interface. For CPC/PLGA/BG, the fibrous capsule was in close contact with the implant surface without the presence of macrophages or multi-nucleated giant cells.

3.4. Quantitative histological evaluation of subcutaneous implants

Two weeks after implantation, statistical analysis of the quantitative histological data revealed a significantly thicker capsule for CPC/PLGA compared to all other formulations (Fig. 5A; $p < 0.05$). In addition, a significantly more mature capsule and interface were

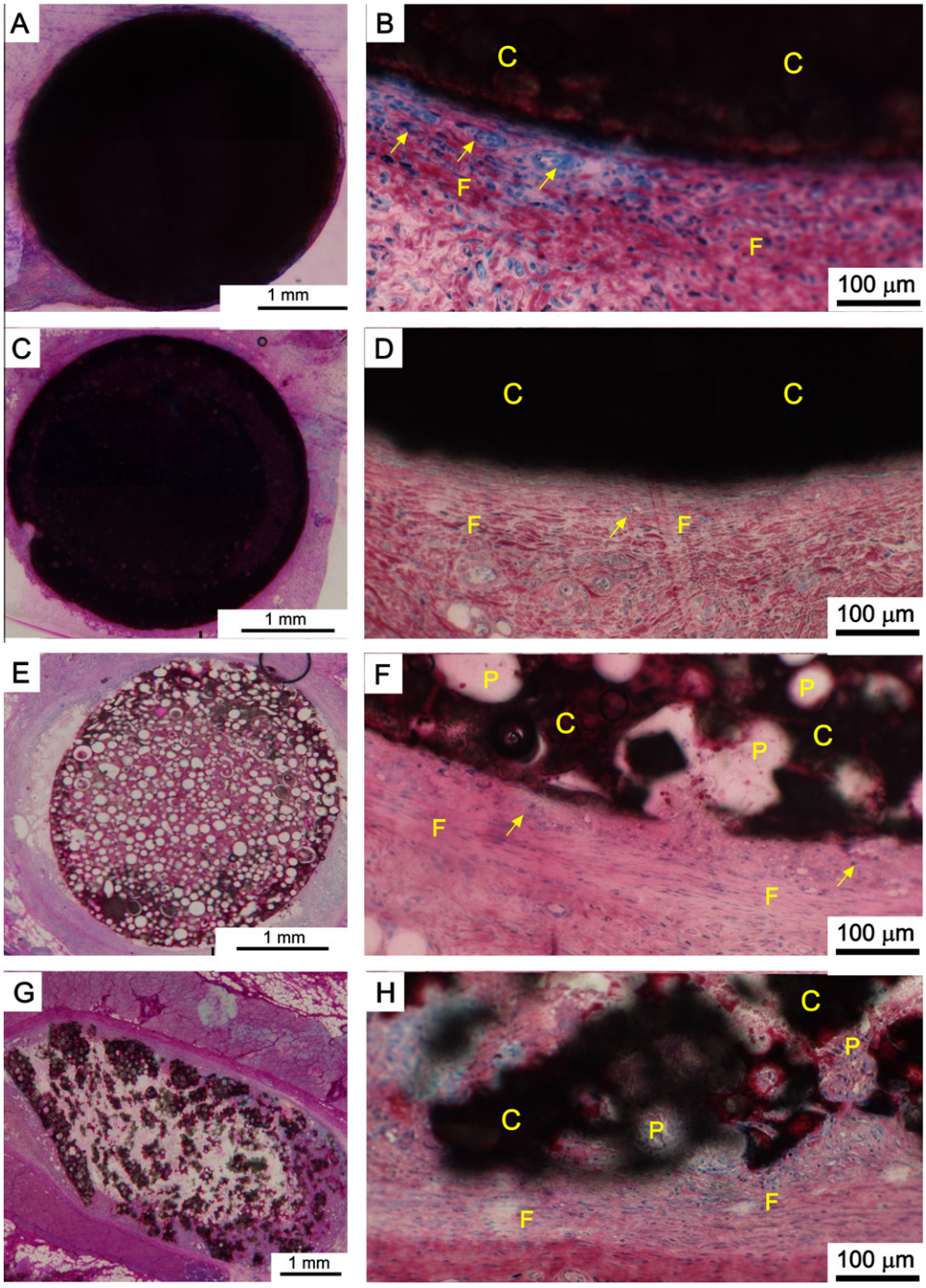

Fig. 3. Representative histological sections of subcutaneous implants of the four experimental groups after two weeks of implantation: CPC (A and B), CPC/BG (C and D), CPC/PLGA (E and F) and CPC/PLGA/BG (G and H). Bar represents 1 mm. Composite material (C), fibrous tissue (F), degraded PLGA pores (P) and multi-nucleated giant cells (arrows) are indicated in the sections. Bar represents 100 μm. Methylene blue and basic fuchsin staining.

observed for CPC/BG and CPC/PLGA/BG compared to CPC/PLGA (Fig. 5B and C, respectively; $p < 0.05$). With increasing implantation time, the capsule thickness, capsule quality and interface quality significantly improved for all experimental groups ($p < 0.01$). At 6 weeks, a significantly thinner capsule surrounding CPC/PLGA/BG was observed compared to CPC and CPC/BG (Fig. 5A; $p < 0.05$). Moreover, the quality of the capsule and interface was significantly more mature for CPC/BG/PLGA compared to CPC and CPC/BG (Fig. 5B and C, respectively; $p < 0.05$).

3.5. Descriptive histology of femoral condyle implants

3.5.1. Two weeks

An overview of representative histological sections of all experimental groups after a 2 week implantation period is depicted in Fig. 6. Although the majority of the implants within the femoral condyle defect were placed correctly, implantation was occasionally imprecise as the bone defect crossed the growth plate, or somewhat too much toward the edge of the femoral condyle.

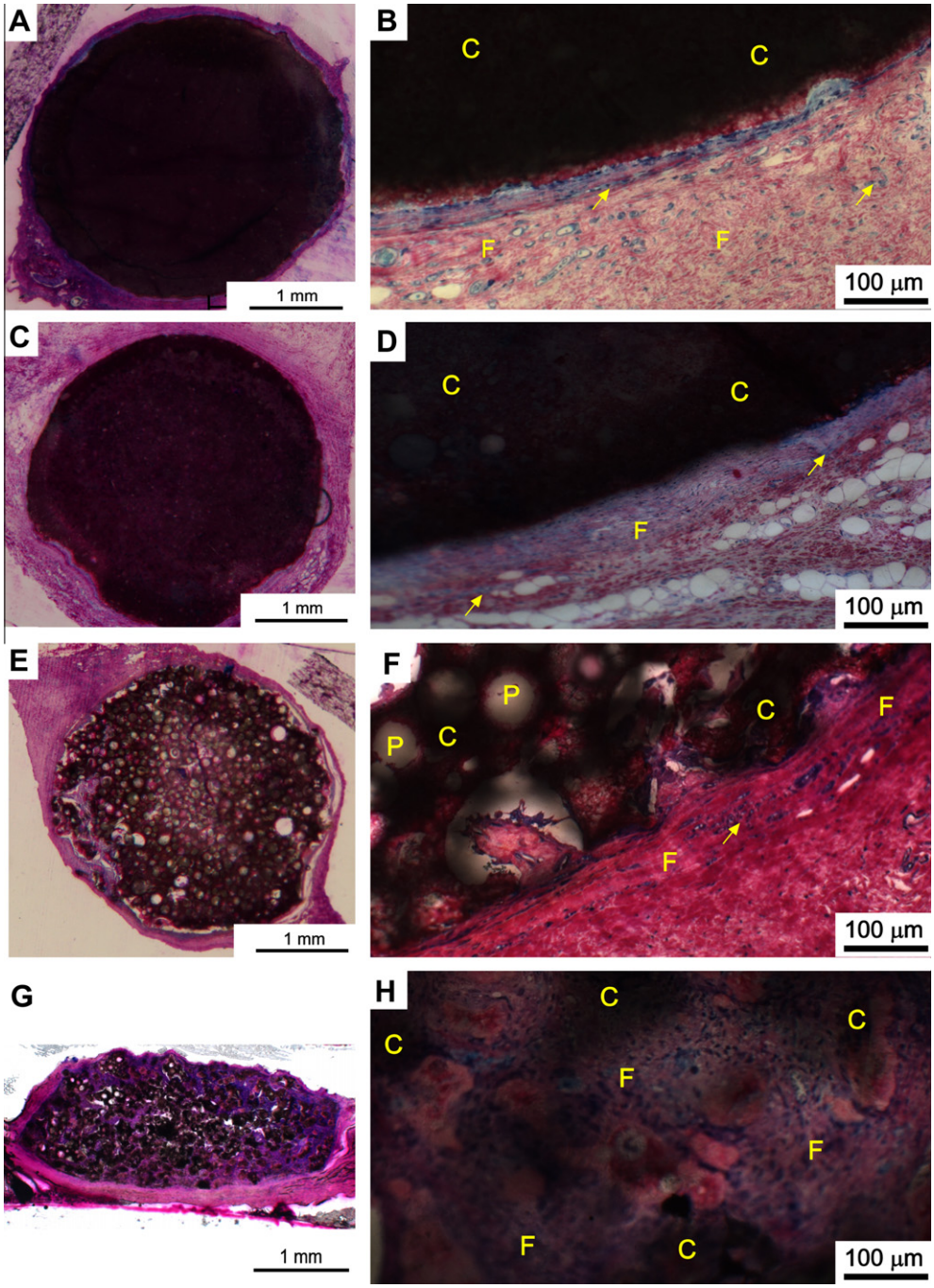

Fig. 4. Representative histological sections of subcutaneous implants of the four experimental groups after six weeks of implantation: CPC (A and B), CPC/BG (C and D), CPC/PLGA (E and F) and CPC/PLGA/BG (G and H). Bar represents 1 mm. Composite material (C), fibrous tissue (F), degraded PLGA pores (P) and multi-nucleated giant cells (arrows) are indicated in the sections. Bar represents 100 µm. Methylene blue and basic fuchsin staining.

Both CPC and CPC/BG showed no signs of degradation, but rather a tight interaction with the surrounding bone (Fig. 6A–D). For CPC/PLGA, the integrity of the implant was slightly affected peripherally, with soft tissue in the contact area between the edges of the bone defect and the implant. Limited newly formed bone was observed in the periphery of the implant (Fig. 6E and F). For CPC/PLGA/BG, the integrity of the implant was completely affected. Degradation of the material allowed the ingrowth of soft tissue accompanied by some bone formation in the central defect region. The region between the implant and the edges of the original defect was either filled with soft tissue or a close contact between bone tissue and implant was observed throughout the degraded material (Fig. 6G and H).

3.5.2. Six weeks

An overview of representative histological sections of all experimental groups after a 6 week implantation period is depicted in Fig. 7.

A limited degradation at the peripheral area of the implants was noticed for CPC. In the contact area between the defect border and CPC, fibrous tissue was observed and, occasionally, bone remodeling was found (Fig. 7A and B). For CPC/BG, very limited degradation

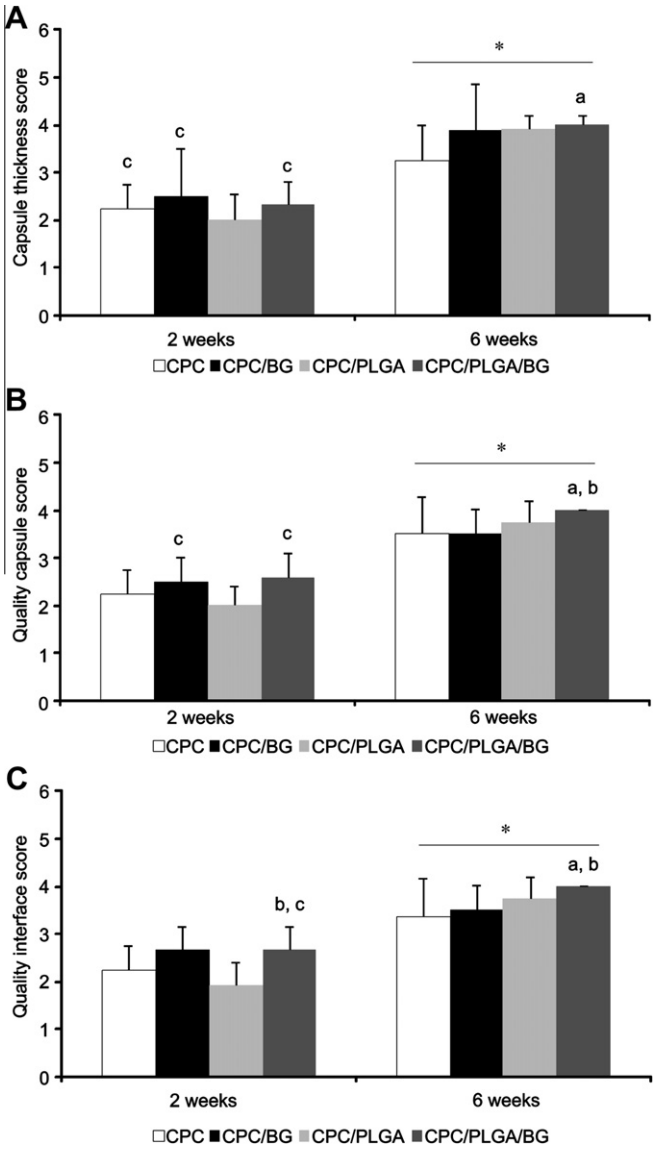

Fig. 5. Histological evaluation of capsule thickness (A), the quality of the capsule (B) and the quality of the interface (C) of the different subcutaneous implants, i.e. CPC, CPC/BG, CPC/PLGA and CPC/PLGA/BG after 2 and 6 weeks implantation using the histological grading scale. Error bars represent means ± standard deviation. (a) $p < 0.05$ compared to CPC; (b) $p < 0.05$ compared to CPC/BG; (c) $p < 0.05$ compared to CPC/PLGA; (∗) $p < 0.05$ compared to 2-weeks equivalent.

of the material was seen in the peripheral region of the implant, with newly formed bone in the areas where CPC/BG had degraded (Fig. 7C and D). For CPC/PLGA, material degradation had continued, leaving lower amounts of material in the defect area compared to the 2 week implantation period. Moreover, in the created PLGA pores located in the central region of the implants soft tissue and some bone ingrowth was observed. The peripherally located PLGA pores were always filled with bone tissue (Fig. 7E and F). The degradation of CPC/PLGA/BG had continued and the material was almost completely degraded after 6 weeks. In addition, throughout the defect area bone ingrowth was found (Fig. 7G and H).

3.6. Histomorphometry of tissue response to femoral condyle implants

3.6.1. Scaffold degradation

Quantitative results on scaffold degradation are presented in Fig. 8A. After 2 weeks of implantation, CPC/PLGA and CPC/PLGA/BG revealed significantly lower amounts of material within the ROI compared to CPC and CPC/BG ($p < 0.05$). With increasing implantation time, CPC/BG, CPC/PLGA and CPC/PLGA/BG showed significantly more scaffold degradation ($p < 0.05$), while no temporal differences were observed for CPC. At 6 weeks, the material amount for CPC/BG, CPC/PLGA and CPC/PLGA/BG were significantly lower compared to CPC ($p < 0.05$). In addition, the amount of material for CPC/PLGA/BG was significantly decreased compared to CPC/BG and CPC/PLGA. No differences were observed between CPC/BG and CPC/PLGA ($p = 0.75$; the amount of material in ROI ranged for CPC from 92 ± 4% to 96 ± 4% after 6 weeks; for CPC/BG from 78 ± 9% to 52 ± 2% after 6 weeks; for CPC/PLGA from 56 ± 13% to 47 ± 2% after 6 weeks; for CPC/PLGA/BG from 35 ± 14% to 10 ± 3% after 6 weeks).

3.6.2. Bone formation

Quantitative results on bone formation within the ROI are depicted in Fig. 8B. After 2 weeks of implantation, no significant differences in bone formation were observed between the different scaffolds. With increasing implantation time, the amount of bone for CPC/BG, CPC/PLGA and CPC/PLGA/BG had significantly increased ($p < 0.05$). At 6 weeks, histomorphometrical analysis revealed significantly more bone formation for CPC/PLGA/BG compared to the other formulations ($p < 0.05$) as well as for CPC/BG and CPC/PLGA compared to CPC ($p < 0.05$; the amount of bone formation ranged for CPC from 6 ± 4% to 13 ± 4% after 6 weeks; for CPC/BG from 11 ± 4% to 29 ± 3% after 6 weeks; for CPC/PLGA from 6 ± 5% to 32 ± 7% after 6 weeks; for CPC/PLGA/BG from 10 ± 3% to 42 ± 10% after 6 weeks).

4. Discussion

This study aimed to evaluate the effects on in vivo tissue response after incorporating BG into CPC (with or without PLGA microparticles) using subcutaneous implantation and implantation into femoral condyle defects in rats after 2 and 6 weeks. It was hypothesized that the addition of BG would not negatively affect the biocompatibility of CPC and CPC/PLGA and would have a positive effect on the formation of bone. The main findings of the subcutaneous implantation showed that BG incorporation had indeed a favorable effect on soft tissue responses in terms of capsule thickness, capsule quality and interface quality. In addition, the femoral condyle defect model revealed that incorporation of BG into CPC or CPC/PLGA significantly accelerated material degradation and enhanced bone formation.

Severe inflammatory response and tissue irritation caused by biomaterials can result in a delay of healing processes [27]. It is well known that the tissue response to an implanted biomaterial is determined by its chemical composition, which will dictate the intensity of the foreign body reaction and inflammatory process [27]. Several studies demonstrated that CPC, CPC/PLGA and BG alone are non-toxic and biocompatible [6,9,18,26,28–31]. In addition, Lee et al. [32] observed enhanced soft tissue adaption after implantation of titanium implants coated with BG in combination with hydroxyapatite (HA). These findings are in line with the results of the current study, which demonstrated that CPC, either pure or combined with PLGA microparticles and/or BG, does not evoke any severe inflammatory responses. Moreover, in the early post-implantation period, the incorporation of BG into CPC or CPC/PLGA provoked a milder soft tissue response, evidenced by a thinner fibrous capsule with a better interface. With increasing implantation time, the different CPC formulations facilitated a relatively mild soft tissue reaction with the superiority for the CPC formulation with BG incorporated into CPC/PLGA. This phenomenon is likely associated with obtaining a balanced pH induced by the addition of BG to the CPC and CPC/PLGA, similar to the observations of Bohner and Matter for brushite

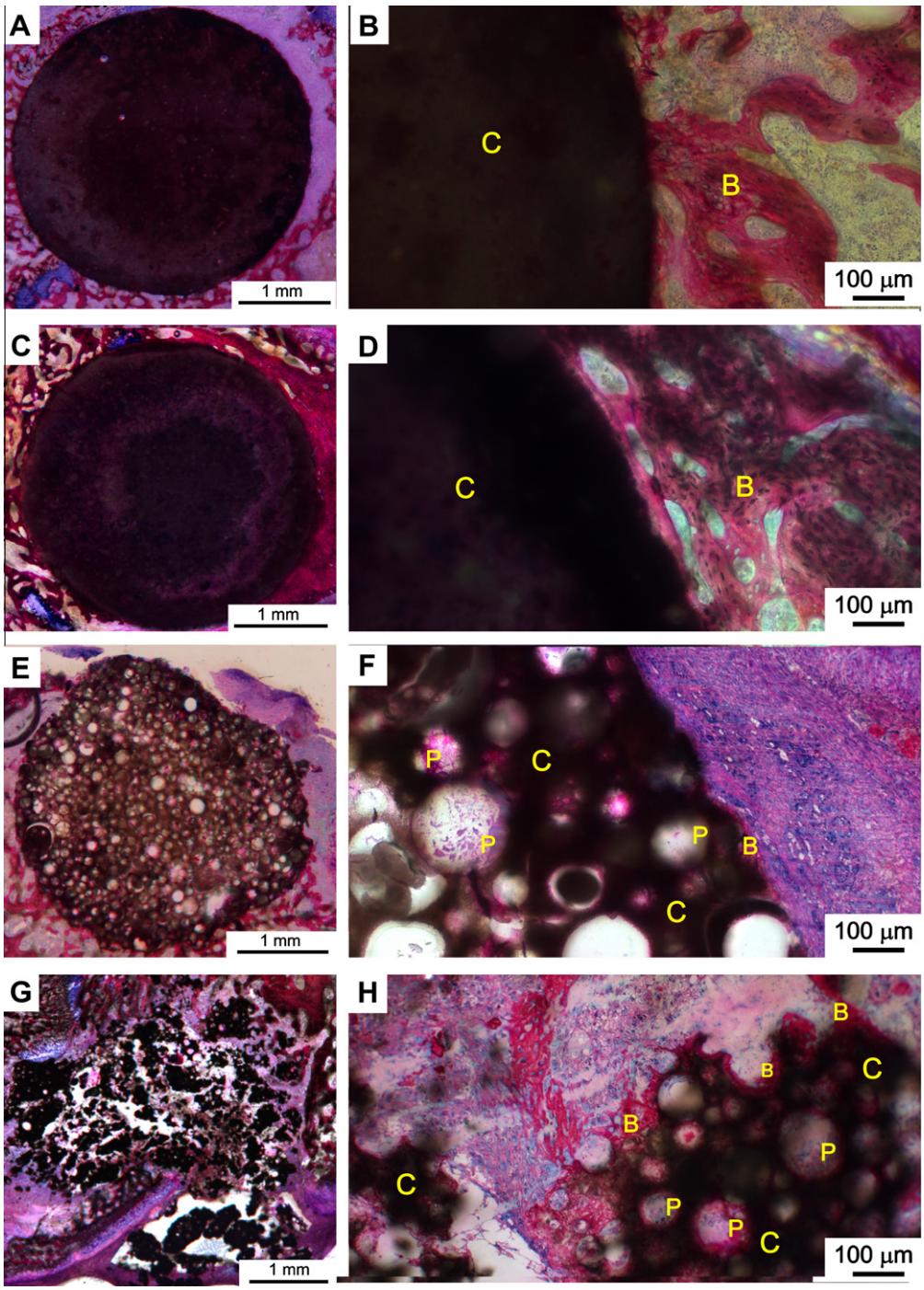

Fig. 6. Representative histological sections of four experimental groups after 2 weeks of implantation in the femoral condyle defect: CPC (A and B), CPC/BG (C and D), CPC/PLGA (E and F) and CPC/PLGA/BG (G and H). Bar represents 1 mm. Composite material (C), bone formation (B) and degraded PLGA pores (P) are indicated in the sections. Bar represents 100 μm. Methylene blue and basic fuchsin staining.

cements [22]. It is well documented that PLGA degradation results in an acidic environment, with the release of lactic and glycolic acid monomers [3,10]. Therefore, PLGA is often combined with other materials that can neutralize excessive acidification and, in turn, reduce the potential adverse tissue response [3,10]. By combining CPC/PLGA with BG, the acidic and basic degradation products counteracted each other, resulting in a more adequate biological environment to support cell proliferation and tissue ingrowth [29].

For the replacement of bone, resorption of the bone substitute material (e.g. biodegradation of the material) is required, since formation of new bone tissue and ingrowth thereof in the defect area needs the liberation of space [28,33,34]. The results of the current study indicate that the degradation rate of the material indeed substantially influences the formation of bone, as with increasing implant degradation higher amounts of newly formed bone were observed. The inclusion of dense PLGA microparticles within CPC has been previously demonstrated to result in accelerated CPC degradation and hence bone formation (i.e. from week 2 onward) due to the release of lactic and glycolic acidic monomers, which produce an acidic environment that acts as a stimulus for CPC

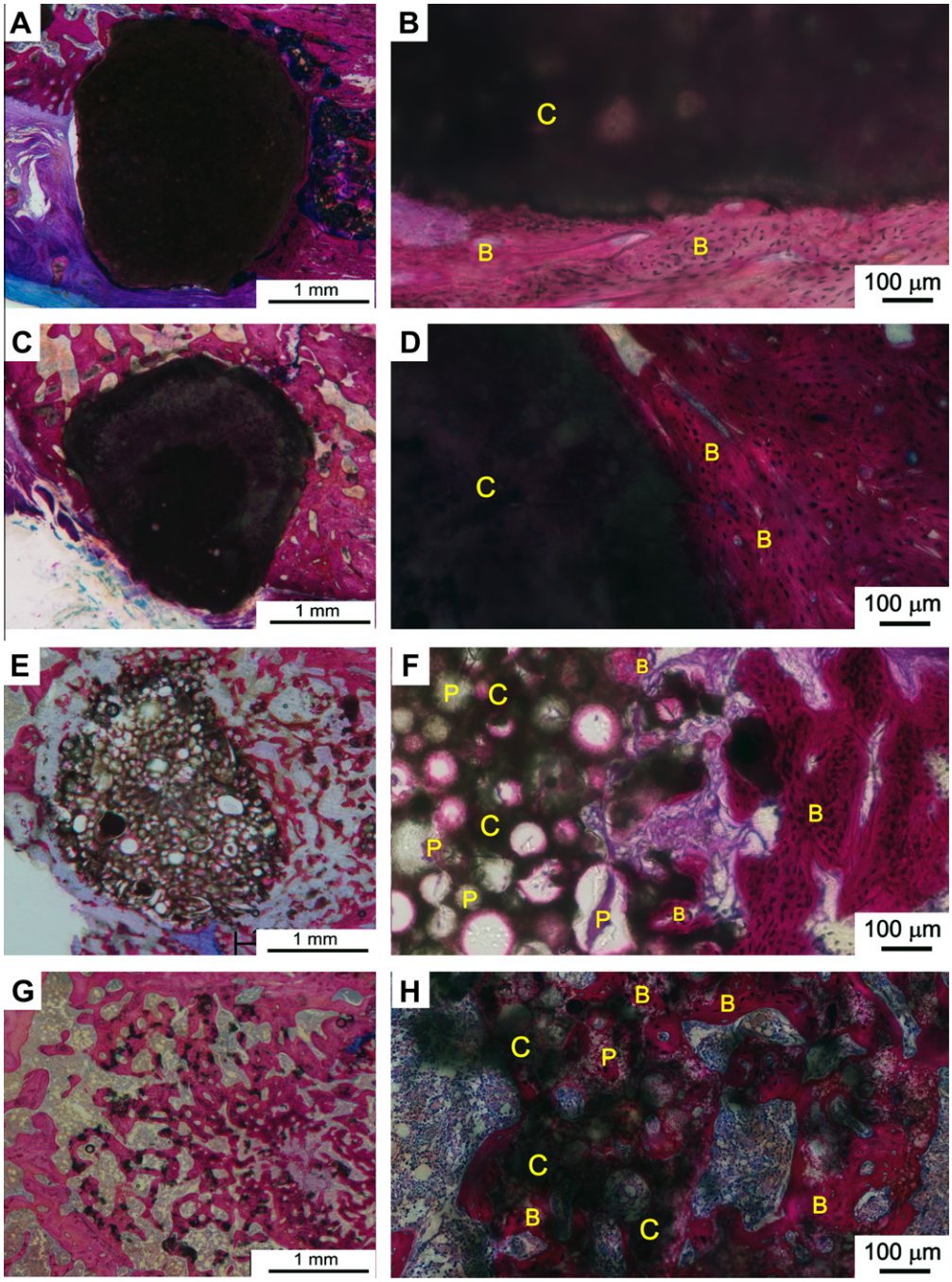

Fig. 7. Representative histological sections of four experimental groups after 6 weeks of implantation in the femoral condyle defect: CPC (A and B), CPC/BG (C and D), CPC/PLGA (E and F) and CPC/PLGA/BG (G and H). Bar represents 1 mm. Composite material (C), bone formation (B) and degraded PLGA pores (P) are indicated in the sections. Bar represents 100 µm. Methylene blue and basic fuchsin staining.

dissolution [3,9]. The increased implant degradation observed for BG-supplemented CPC might be related to the increased BG dissolution immediately after contact with fluids [34–36], resulting in a lower amount of remaining implant material at an earlier time point compared to the slow degradable pure CPC. It is likely that the superior biological performance of BG combined with PLGA-microparticles-supplemented CPC is determined by the positive effects of both BG and PLGA on the material degradation.

Additionally, upon implantation, ionic dissolution products of BG have been shown to beneficially affect osteogenesis by formation of a silica-rich layer, which can act as a template for calcium phosphate precipitation and direct new bone formation [14–18]. Furthermore, it has been reported that BG has a stimulatory effect on neovascularization by stimulating the secretion of angiogenic factors [35,37], which together with the osteopromotive properties of BG might further influence bone formation when using BG-supplemented CPC, either pure or supplemented with PLGA. However, the current study addressed the effect of BG inclusion in CPC based on histological analysis rather than at cell level. Consequently, direct evidence of osteopromotion and angiogenesis by BG is not available from the current study. Nevertheless, the outcome of the current study confirmed our hypothesis that BG can improve the biological performance of CPC and CPC/PLGA after 6 weeks of implantation. Consequently, BG-supplemented CPC might be promising to improve the performance

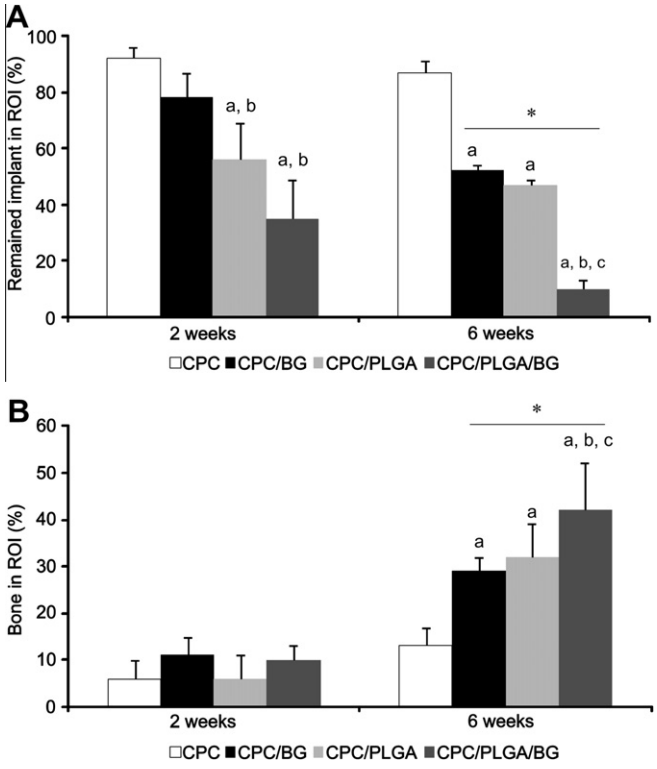

Fig. 8. Results of histomorphometrical evaluation of the different formulations, i.e. CPC, CPC/BG, CPC/PLGA and CPC/PLGA/BG. (A) The amount of remained implant and (B) the amount of newly formed bone after 2 and 6 weeks are expressed as percentage of ROI (i.e. a standardized region of interest with similar dimensions as created defect). Error bars represent means ± standard deviation. (a) $p < 0.05$ compared to CPC; (b) $p < 0.05$ compared to CPC/BG; (c) $p < 0.05$ compared to CPC/PLGA; (∗) $p < 0.05$ compared to 2-weeks equivalent.

of CPC required for compromised conditions. However, in view of the differences in bone metabolism in healthy bone compared to compromised conditions (e.g. osteoporosis), the biological performance of BG-supplemented CPC might be different. As this study was limited to relatively short-term evaluation of the performance of preset BG-supplemented CPC under optimal conditions to provide full control over the complete filling of the defect, information on the long-term performance of the (injectable) material and under compromised conditions remains to be provided.

In conclusion, BG incorporation into CPC (or CPC/PLGA) improved the soft tissue response upon ectopic implantation compared to pure CPC (or CPC/PLGA). In addition, incorporating BG within CPC accelerated material degradation and increased bone formation in a femoral condyle defect in rats. Consequently, these data highlight the potential of BG to be used as an additive to CPC to improve the biological performance for bone regeneration applications. Further long-term studies should be carried out to provide additional information concerning the late stages of material degradation and bone regeneration induced by the CPC/PLGA cements including BG. In addition, further research is required to evaluate the biological performance of BG-supplemented CPC in compromised situations.

Acknowledgements

The authors gratefully acknowledge the support of the Smart Mix Program of the Netherlands Ministry of Economic Affairs and The Netherlands Ministry of Education, Culture and Science. The authors would like to thank Natasja van Dijk for assistance with the histological preparations. Scanning electron microscopy was performed at the Nijmegen Center for Molecular Life Sciences (NCMLS), The Netherlands.

Appendix A. Figures with essential colour discrimination

Certain figures in this article, particularly Figs. 1, 3, 4, 6 and 7, are difficult to interpret in black and white. The full colour images can be found in the on-line version, at http://dx.doi.org/10.1016/j.actbio.2012.11.009.

References

[1] Habraken WJEM, Wolke JGC, Jansen JA. Ceramic composites as matrices and scaffolds for drug delivery in tissue engineering. Adv Drug Deliv Rev 2007;59:234–48.
[2] Bodde EWH, Habraken WJEM, Mikos AG, Spauwen PHM, Jansen JA. Effect of polymer molecular weight on the bone biological activity of biodegradable polymer/calcium phosphate cement composites. Tissue Eng Part A 2009;15:3183–91.
[3] Félix Lanao RP, Leeuwenburgh SCG, Wolke JGC, Jansen JA. In vitro degradation rate of apatitic calcium phosphate cement with incorporated PLGA microspheres. Acta Biomater 2011;7:3459–68.
[4] Liao H, Walboomers XF, Habraken WJEM, Zhang Z, Li Y, Grijpma DW, et al. Injectable calcium phosphate cement with PLGA, gelatin and PTMC microspheres in a rabbit femoral defect. Acta Biomater 2011;7:1752–9.
[5] Habraken WJEM, Wolke JGC, Mikos AG, Jansen JA. PLGA microsphere/calcium phosphate cement composites for tissue engineering: in vitro release and degradation characteristics. J Biomater Sci Polym Ed 2008;19:1171–88.
[6] Bodde E, Cammaert C, Wolke J, Spauwen P, Jansen J. Investigation as to the osteoinductivity of macroporous calcium phosphate cement in goats. J Biomed Mater Res B 2007;83B:161–8.
[7] Ruhé P, Boerman O, Russel F, Mikos A, Spauwen P, Jansen J. In vivo release of rhBMP-2 loaded porous calcium phosphate cement pretreated with albumin. J Mater Sci Mater Med 2006;17:919–27.
[8] Lonink DP, van den Dolder J, van den Beucken JJJP, Cuijpers VM, Wolke JGC, Mikos AG, et al. Evaluation of the biocompatibility of calcium phosphate cement/PLGA microparticle composites. J Biomed Mater Res A 2008;87A:760–9.
[9] Félix Lanao RP, Leeuwenburgh SCG, Wolke JGC, Jansen JA. Bone response to fast-degrading, injectable calcium phosphate cements containing PLGA microparticles. Biomaterials 2011;32:8839–47.
[10] Habraken W, Wolke J, Mikos A, Jansen J. Injectable PLGA microsphere/calcium phosphate cements: physical properties and degradation characteristics. J Biomater Sci Polym Ed 2006;17:1057–74.
[11] Ruhé P, Hedberg E, Padron NT, Spauwen P, Jansen J, Mikos A. RhBMP-2 release from injectable poly(D,L-lactic-co-glycolic acid)/calcium-phosphate cement composites. J Bone Joint Surg Am 2003;85:75–81.
[12] Plachokova A, Link D, van den Dolder J, van den Beucken J, Jansen J. Bone regenerative properties of injectable PGLA–CaP composite with TGF-β1 in a rat augmentation model. J Tissue Eng Regen Med 2007;1:457–64.
[13] Bodde E, Boerman O, Russel F, Mikos A, Spauwen P, Jansen J. The kinetic and biological activity of different loaded rhBMP-2 calcium phosphate cement implants in rats. J Biomed Mater Res A 2008;87A:780–91.
[14] Välimäki VV, Aro HT. Molecular basis for the action of bioactive glasses as bone graft. Scand J Surg 2006;95:95–102.
[15] Hench LL, Polak JM. Third-generation biomedical materials. Science 2002;295:1014–7.
[16] Xynos ID, Edgar AJ, Buttery LDK, Hench LL, Polak JM. Ionic products of bioactive glass dissolution increase proliferation of human osteoblasts and induce insulin-like growth factor II mRNA expression and protein synthesis. Biochem Biophys Res Commun 2000;276:461–5.
[17] Hench LL, Xynos ID, Polak JM. Bioactive glasses for in situ tissue regeneration. J Biomater Sci Polym Ed 2004;15:543–62.
[18] Moura J, Teixeira LN, Ravagnani C, Peitl O, Zanotto ED, Beloti MM, et al. In vitro osteogenesis on a highly bioactive glass-ceramic (Biosilicate®). J Biomed Mater Res A 2007;82A:545–57.
[19] Huan Z, Leeflang S, Zhou J, Zhai W, Chang J, Duszczyk J. In vitro degradation behavior and bioactivity of magnesium-Bioglass® composites for orthopedic applications. J Biomed Mater Res B 2012;100B:437–46.
[20] Oonishi H, Hench LL, Wilson J, Sugihara F, Tsuji E, Kushitani S, et al. Comparative bone growth behavior in granules of bioceramic materials of various sizes. J Biomed Mater Res 1999;44:31–43.
[21] Granito RN, Rennó AC, Ravagnani C, Bossini PS, Mochiuti D, Jorgetti V, et al. In vivo biological performance of a novel highly bioactive glass-ceramic (Biosilicate®): a biomechanical and histomorphometric study in rat tibial defects. J Biomed Mater Res B 2011;97B:139–47.
[22] Bohner M, Matter S. Effect of bioglass granules on the physico-chemical properties of brushite cements. Key Eng Mater 2001;192–195:809–12.
[23] Zanotto ED, Ravagnani C, Peitl O, Panzeri H, EH L. Process and compositions for preparing particulate, bioactive or resorbable biosilicates for use in the treatment of oral ailments, WO2004/074199, Fundação Universidade Federal De São Carlos, Universidade De São Paulo, 20 February 2004, Int. C. C03C10/00.

[24] van der Lubbe H, Klein C, de Groot K. A simple method for preparing thin (10 microM) histological sections of undecalcified plastic embedded bone with implants. Stain Technol 1988;63:171–6.
[25] Jansen J, Dhert W, van der Waerden J, von Recum A. Semi-quantitative and qualitative histological analysis method for the evaluation of implant biocompatibillty. J Invest Surg 1994;7:123–34.
[26] Link D, van den Dolder J, van den Beucken J, Cuijpers V, Wolke J, Mikos A, et al. Evaluation of the biocompatibility of calcium phosphate cement/PLGA microparticle composites. J Biomed Mater Res A 2008;87A:760–9.
[27] Anderson J, McNally A. Biocompatibility of implants: lymphocyte/macrophage interactions. Semin Immunopathol 2011;33:221–33.
[28] van de Watering FCJ, van den Beucken JJJP, Walboomers XF, Jansen JA. Calcium phosphate/poly(D,L-lactic-co-glycolic acid) composite bone substitute materials: evaluation of temporal degradation and bone ingrowth in a rat critical-sized cranial defect. Clin Oral Implants Res 2012;23:151–9.
[29] Day RM, Maquet V, Boccaccini AR, Jérôme R, Forbes A. In vitro and in vivo analysis of macroporous biodegradable poly(D,L-lactide-co-glycolide) scaffolds containing bioactive glass. J Biomed Mater Res A 2005;75A:778–87.
[30] Vargas GE, Mesones RV, Bretcanu O, López JMP, Boccaccini AR, Gorustovich A. Biocompatibility and bone mineralization potential of 45S5 Bioglass®-derived glass–ceramic scaffolds in chick embryos. Acta Biomater 2009;5:374–80.
[31] Vogel M, Voigt C, Knabe C, Radlanski RJ, Gross UM, Müller-Mai CM. Development of multinuclear giant cells during the degradation of Bioglass® particles in rabbits. J Biomed Mater Res A 2004;70A:370–9.
[32] Lee JH, Nam H, Ryu HS, Seo JH, Chang BS, Lee CK. Bioactive ceramic coating of cancellous screws improves the osseointegration in the cancellous bone. J Orthop Sci 2011;16:291–7.
[33] Ruhé P, Hedberg E, Padron NT, Spauwen P, Jansen J, Mikos A. Biocompatibility and degradation of poly(D,L-lactic-co-glycolic acid)/calcium phosphate cement composites. J Biomed Mater Res A 2005;74A:533–44.
[34] Qi X, Ye J, Wang Y. Improved injectability and in vitro degradation of a calcium phosphate cement containing poly(lactide-co-glycolide) microspheres. Acta Biomater 2008;4:1837–45.
[35] Hoppe A, Güldal NS, Boccaccini AR. A review of the biological response to ionic dissolution products from bioactive glasses and glass-ceramics. Biomaterials 2011;32:2757–74.
[36] Rahaman MN, Day DE, Sonny Bal B, Fu Q, Jung SB, Bonewald LF, et al. Bioactive glass in tissue engineering. Acta Biomater 2011;7:2355–73.
[37] Gorustovich A, Roether JA, Boccaccini AR. Effect of bioactive glasses on angiogenesis: a review of in vitro and in vivo evidences. Tissue Eng Part B 2010;16:199–207.